ORIGINAL ARTICLE

Synthesis, characterization and catalytic activity of furosemide-functionalized ferrite on the sedimentation behavior of starch

S. Palanikumar · B. Meenarathi ·
L. Kannammal · R. Anbarasan

Abstract Furosemide-functionalized nanoferrite was synthesized and characterized by various analytical techniques. The furosemide-functionalized ferrite was used to settle down the starch particles under three different pH. Thus, obtained starch/Fe_3O_4 nanocomposites were characterized by Fourier transform infrared spectroscopy (FTIR), fluorescence spectroscopy, scanning electron microscopy (SEM), differential scanning calorimetry (DSC) and thermogravimetric analysis (TGA). The sedimentation velocity of starch in the presence of furosemide-functionalized Fe_3O_4 was critically compared with the available literature value and the results are discussed in detail. The high sedimentation velocity of starch under the influence of gravitational force and the external magnetic force is studied. The starch-coated ferrites exhibited the lower vibrating sample magnetometer (VSM) value. This novel research work will bring out a new methodology in the field of starch materials.

Introduction

Food emulsion contains starch and protein as the major component in our daily life. Starch is an important bio-food material for people particularly south Indians as rice and

S. Palanikumar · B. Meenarathi · L. Kannammal ·
R. Anbarasan (✉)
Department of Polymer Technology, Kamaraj College of
Engineering and Technology, Virudhunagar 626001,
Tamil Nadu, India
e-mail: anbu_may3@yahoo.co.in

potato. Such a life saving starch is a biopolymer present in seeds, stems and roots of plants including wheat, barley and corns in the form of minute granules as renewable resources. In most of the industries, starch is extracted from cereal and tubule roots. Various methodologies are adopted for the isolation and purification of starch as mentioned here. For example in 1999, Closs et al. (1999) studied the phase separation and rheologies of starch/galactomannan in an aqueous system. Sajeev et al. (2002) reported the gravity settling velocity of starch in an aqueous suspension. Extraction of cassava starch explained the modality (Da et al. 2010). Sedimentation, microfiltration and reverse osmosis were done for the washing of corn starch (Madariaga and Aquirre 2011), using different ammonium chloride-based flocculants for the isolation of starch from its resource material (Wei et al. 2008). During the isolation and purification of starch larger quantity of water is consumed and, hence, the water resistivity has direct relationship to the chemical potential of water, and hence leads to the degradation of carbohydrates in the starch. It means that during the long sedimentation process, the water molecules slowly degrade the structure of carbohydrate in the presence of water-living microbial system. This type of microbial activity leads to the formation of low-quality starch as well as wasting of starch. It was calculated that around 5 % of starch was wasted by the microbial activities. In order to save such a food material, various methodologies have been used. By thorough literature survey, we could not find any report based on the magnetic sedimentation of starch molecules.

The nanosized iron oxide has many unique properties such as high coercivity, low curie temperature and high magnetic susceptibility values with excellent superparamagnetism. Such a nice candidate can be synthesized by different methods (Sun et al. 2007; Prakash et al. 2004;

Li et al. 2005; Bin et al. 2009; Tian et al. 2010). Recently, the magnetic nanoparticles are found to have important biomedical applications such as MRI agent (Huang and Juang 2011; Mos et al. 2007), detection of biological cavities (He et al. 2005), etc. Due to the absence of surface of functionalities, the applications of magnetic nanoparticles are restricted to some extent. This problem can be outwitted by the functionalization process. Fe_3O_4 nanoparticles were functionalized by propargyl acid (Zhou et al. 2008), dimercaptosuccinic acid (Kim et al. 2010), oleic acid (Xiao et al. 2010), ethylenediamine (Gang et al. 2010), streptavidin (Koussi et al. 2007), daunomycin (Chen et al. 2008), polystyrene (Jiang et al. 2007) and oleylamine (Klokkenburg et al. 2007). On thorough literature survey, we could not find any report based on furosemide-functionalized Fe_3O_4 nanoparticle. The novelty of the present investigation is that furosemide-functionalized Fe_3O_4 nanoparticle was synthesized by co-precipitation method and the same was used for the sedimentation of starch particles.

Functionalization of Fe_3O_4 by furosemide is simply a surface reaction. Furosemide contains one NH_2, SO_2, CO_2H, NH, ether and one Cl atom. The NH group of furosemide interacts with the Fe_3O_4 surface. The OH group of starch can interact either with the amino group or SO_2 or ether linkage through secondary forces of attraction. Furosemide offers more functionalities for starch molecules. The OH group of starch can interact with any of the functional groups of furosemide.

Experimental

Materials

The raw materials required for the preparation of Fe_3O_4 nanoparticles are as follows: ferrous sulfate ($FeSO_4$), ferric chloride ($FeCl_3$) and sodium hydroxide (NaOH) were purchased from CDH, India. The double distilled (DD) water was used for the solution preparation work. The ferrite nanoparticle was functionalized in the presence of furosemide (Ranbaxy, India). The sedimentation velocity of starch (purchased from Himedia chemicals, India) was studied under three different pH values at 2.5, 7.1 and 12.0.

Synthesis of ferrite and furosemide-functionalized ferrite

In the first step, pristine ferrite nanoparticles were synthesized by the co-precipitation method. The procedure is given below: 5-g ferrous sulfate in 50-mL DD water was taken in a 250-mL round bottom (RB) flask. 10-g ferric chloride in 50-mL water was added slowly into the RB flask. The slow addition was continued for 30 min at 45 °C
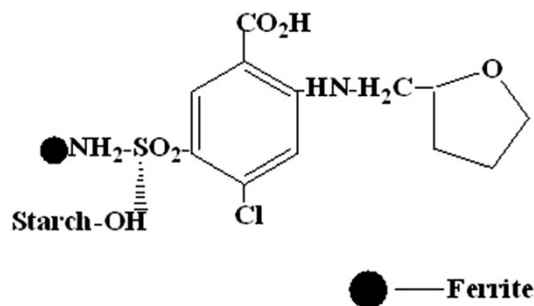
Scheme 1 .

under nitrogen atmosphere under mild stirring condition. After the complete mixing, the temperature of the reaction system was reduced to room temperature with the simultaneous addition of 1 M NaOH solution under vigorous stirring. While adding sodium hydroxide, the nucleation process started and there is a formation of ferrite nanocrystals (Koussi et al. 2007). The ferrite formation can be confirmed by the appearance of the black coloration while adding NaOH solution. Now the pH was adjusted to 12.5. After 2 h of nucleation reaction, the contents were stirred for another 1 h. At the end of the reaction, the contents were transferred to a 500-mL beaker and the same was kept on a magnetic bar. After a certain period of time, the black color precipitate settled down and the supernatant liquid was removed by pipetting without any disturbance in the medium. Thus, the obtained black-colored precipitate was washed thrice with 100-mL DD water. This process was repeated to remove the impurities from the system. After the complete removal of water, the ferrite nanoparticles were dried at 110 °C for 8 h. Thus, obtained fine black powder of ferrite was weighed and stored in a zipper lock bag. In the second step, the furosemide-functionalized ferrite nanoparticle was synthesized. Here also one can follow the above-mentioned procedure but in the presence of 2-g furosemide in 20-mL DD water.

2-g potato starch was dissolved in 100-mL DD water. The above-synthesized furosemide-decorated ferrite nanoparticles were added slowly under vigorous stirring condition. The furosemide-functionalized ferrite can be loaded at different percentage weight. After the reaction, the contents were evaporated to dryness. The final product, starch/furosemide-functionalized ferrite nanoparticle systems were dried, weighed and stored in a zipper lock cover.

Fe_3O_4 is a biocompatible nano metal oxide. It is sensitive towards the applied magnetic force. For 2 g of starch, 0.01 g of furosemide-functionalized Fe_3O_4 was added (0.5 %). This is a negligible amount when compared with the amount of starch. It is also used to improve the iron content in the human body. It is used to improve the mechanical strength of the bones and teeth of humans.

Hence, it is not necessary to remove the Fe_3O_4 from the starch after its isolation from the medium.

Characterization

FTIR spectrum was taken using Shimadzu 8400 S, Japan model instrument from 4,000 to 400 cm^{-1} by KBr pellet-ization method. Jasco V-570 instrument was used for UV–visible spectrum measurements. 2-mg sample was dissolved in 10-mL DD water under ultrasonic irradiation for 10 min and subjected to UV–visible spectral measurements. Fluorescence spectrum (excited at 290 nm) was measured with the help of Jasco Model FP-6000, Japan, instrument from 300 to 700 nm. X-ray diffraction (XRD, XS08, Bruker, USA) was recorded with an advanced instrument and scanning from the 2θ value of 10°–80° at a scanning rate of 2°/min. The surface morphology of the samples was scanned by SEM (JSM 6300, JEOL model) instrument. Magnetic measurements were carried out with a superconducting quantum interference device magnetometer (Lakesore-7410-VSM, USA) with magnetic fields up to 7 T at 32 °C.

Sedimentation study

The settling velocity of starch in the presence of furosemide-functionalized ferrite nanoparticle under three different pH was determined using the following formula (Sajeev et al. 2002).

$$v_0 = \frac{g d_s^2 (\rho_s - \rho_w)}{18 \mu_w}$$

where V_0 is free-falling velocity in m s^{-1}, g acceleration due to gravity in m s^{-2}, d_s diameter of starch particle, ρ_s density of starch particle in kg m^{-3}, ρ_w density of water in kg m^{-3}, and μ_w viscosity of water in kg m^{-1} s^{-1}.

Results and discussion

For the sake of convenience, the present results and discussion part is sub-divided into two parts namely, (1) characterizations of furosemide-functionalized ferrite nanoparticles, (2) characterizations of ferrite–furosemide–starch nano composites.

Characterizations of furosemide-functionalized ferrite nanoparticles

FTIR study

The functional groups present in the ferrite before and after functionalization can be determined by FTIR spectroscopy.
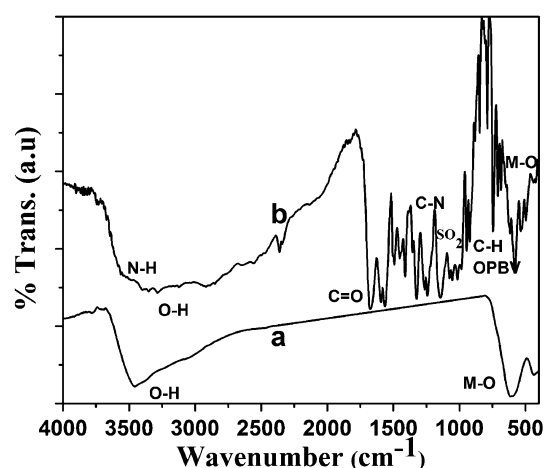

Fig. 1 FTIR spectrum of **a** pristine ferrite, **b** furosemide-functionalized ferrite

A broad peak around 3,500 cm^{-1} (Fig. 1a) explains the –OH stretching. The –OH stretching is due to the intercalated water molecules. The M–O stretching is observed at 608 cm^{-1} (Gang et al. 2010). In the case of pristine ferrite, one can see the OH and M–O stretching alone. Figure 1b indicates the furosemide-functionalized ferrite. The N–H stretchings are observed at 3,454 cm^{-1}. This is in accordance with Gang et al. (2010). The SO_2 stretchings are observed around 1,015 cm^{-1}. The C–N stretching can be seen at 1,328 cm^{-1}. The C=O stretching of carboxyl group appeared at 1,676 cm^{-1}. The cyclic C–O–C ether linkage and C–H out of plane bending vibration can be seen at 1,138 and 749 cm^{-1}, respectively. The M–O stretching is observed at 570 cm^{-1}. Thus, the FTIR spectrum confirms the functionalization of ferrite by furosemide.

UV–visible spectroscopy

Figure 2a represents the UV–visible spectrum of pristine ferrite which exhibits one broad peak at 380 nm corresponding to the ferrite. After the surface functionalization of ferrite, the spectrum exhibits two sharp peaks at 327 and 274 nm (Fig. 2b). A peak at 274 nm is associated with the $\pi \rightarrow \pi^*$ transition of phenyl ring present in the furosemide. Ferrites are observed at 327 nm. On comparison, the peak corresponding to ferrite is blue shifted due to the surface functionalization and size reduction of ferrite. Ahmad et al. (2009) reported the UV–visible spectrum of ferrite with an absorption peak at 410 nm. But in the present investigation due to the size reduction of ferrite and the encapsulation of ferrite by furosemide, the absorption peak is blue shifted. Figure 2c confirms the fluorescence spectrum of pristine ferrite at 377 nm with the intensity value of 7.3 cps. Figure 2d declares the
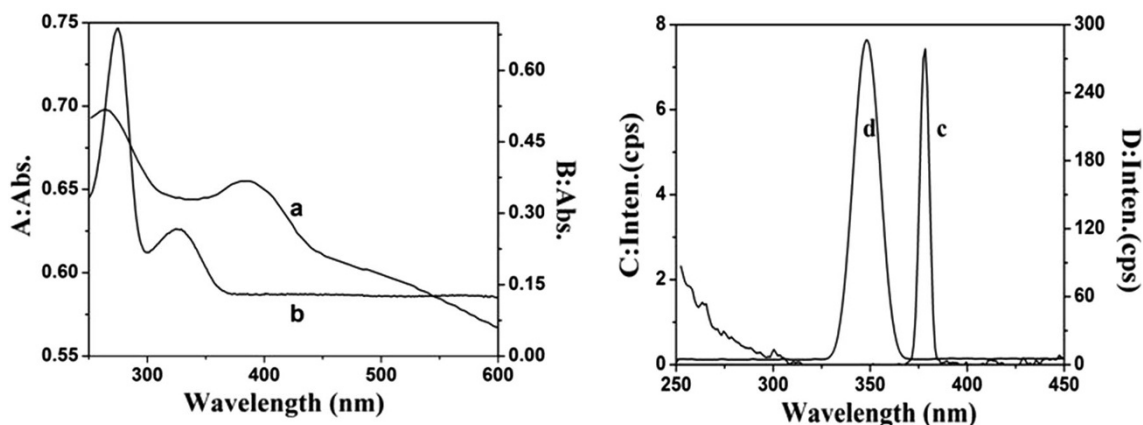
Fig. 2 UV–visible spectrum of **a** pristine ferrite, **b** furosemide-functionalized ferrite and fluorescence emission spectrum of **c** pristine ferrite, **d** furosemide-functionalized ferrite
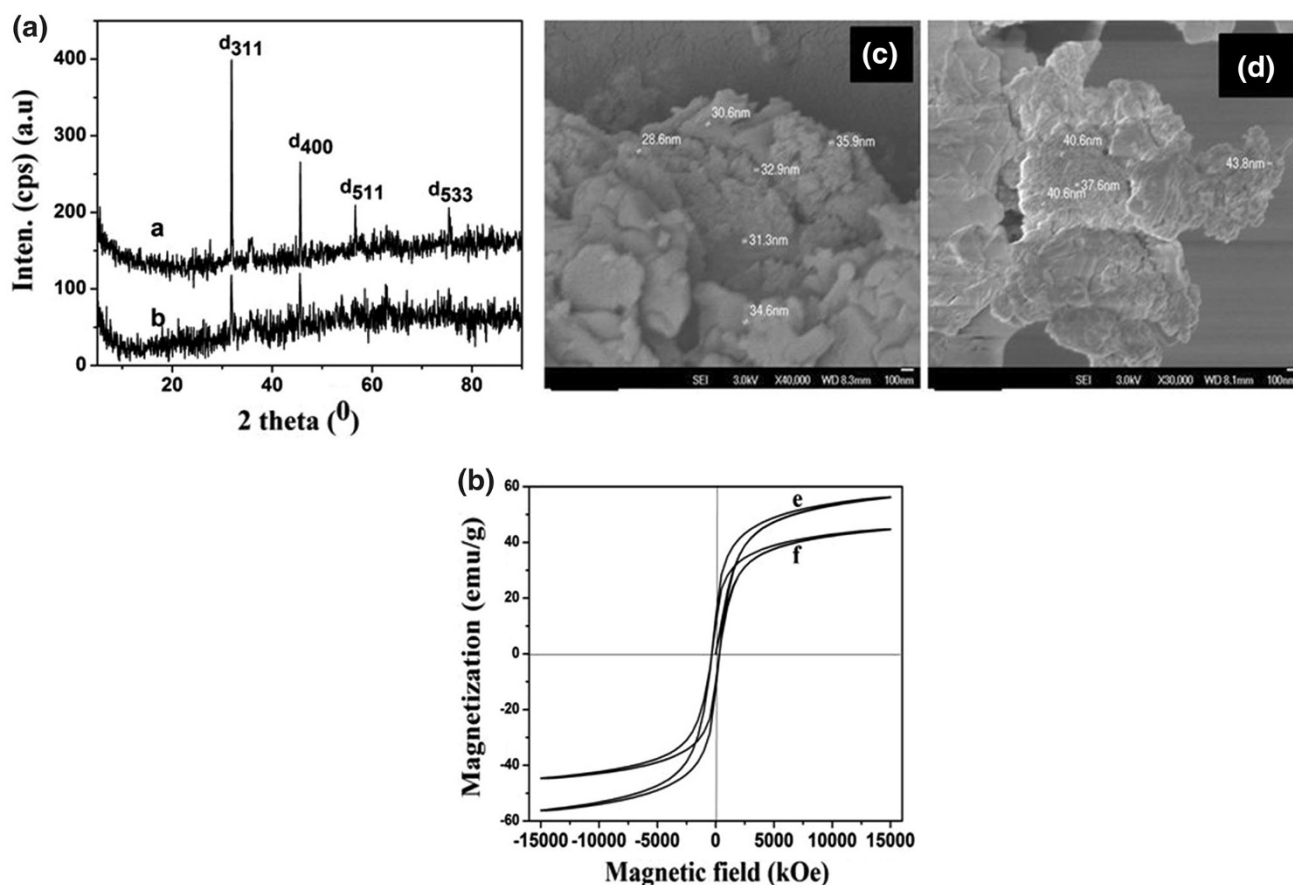

Fig. 3 XRD of **a** pristine ferrite, **b** furosemide-functionalized ferrite, **c**, **d** FESEM images of furosemide-functionalized ferrite and VSM loop of **e** pristine ferrite, **f** furosemide-functionalized ferrite

fluorescence emissions spectrum of ferrite after functionalization with furosemide at 347 nm with the fluorescence emission intensity (FEI) of 292 cps. On comparison, the ferrite after functionalization with furosemide exhibits high FEI value. The increase in intensity is associated with the surface functionalization of ferrite with furosemide.

XRD profile

Figure 3a, b enumerates the XRD of ferrite before and after functionalization with furosemide. The pristine ferrite (Fig. 3a) exhibits d_{311}, d_{400}, d_{511} and d_{533} crystal planes at 31.8°, 45.6°, 56.7° and 75.3°, respectively (Ahmad et al. 2009). The ferrite after functionalization with furosemide

exhibits the same crystal planes corresponding to the ferrite, but with lesser intensity (Fig. 3b). This can be explained as follows. (1) due to the surface functionalization, (2) the furosemide may intercalate into the basal spacing of ferrite. The XRD results indicate that there is no change in the peak position, which indicates that during the functionalization process there is no delamination or exfoliation of ferrite crystals. It seems that the added furosemide is simply adsorbed on the surface of ferrite. Due to the surface functionalization reaction, the crystallinity of ferrite was disturbed and becomes amorphous. The decrease in crystallinity of ferrite strongly infers that there exists a stable interaction between ferrite and furosemide. Furosemide contains one NH_2, SO_2, CO, NH and Cl group. Among those, amino group is a good metal oxide surface binding group.

FE–SEM analysis

Figure 3c, d indicates the FE–SEM of furosemide-functionalized ferrite. Here, the size of the ferrite was calculated as 35 nm approximately with agglomerated structure. This result reveals that the added furosemide simply adheres on the surface of the ferrite.

VSM measurement

Figure 3 shows the VSM loops of ferrite before and after functionalization with furosemide. The pure ferrite (Fig. 3e) exhibits the VSM value of 53.4 emu/g, whereas ferrite after functionalization with furosemide (Fig. 3f) exhibits the VSM value of 42.7 emu/g. The decrease in magnetization value is ascribed to the surface adsorption of furosemide. Due to the surface functionalization reaction, the added furosemide is coated on the surface of ferrite like a thin film. As a result of encapsulation, the magnetisation value of ferrite was depressed. In 2008, Vinod et al. (2008) studied the VSM of ferrite before and after encapsulation with poly(diacetylene) molecules. They reported that after the encapsulation of ferrite with poly(diacetylene) chains, the VSM value was reduced. Our result is in accordance with their report. In the present investigation, ferrite after the surface functionalization with furosemide the VSM value was decreased. Similar type of observation was noted by Aouak et al. (2013).

Characterizations of ferrite–furosemide–starch nano composites

FTIR study

The FTIR spectrum explains the functional groups present in the system. Figure 4a shows the FTIR
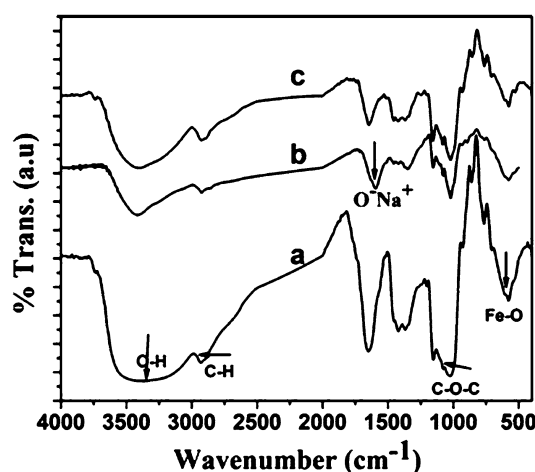

Fig. 4 FTIR spectrum of ferrite–furosemide–starch prepared under **a** acidic pH, **b** alkaline pH, **c** neutral pH

spectrum of Fe_3O_4–furosemide–starch prepared under acidic pH. The –OH bending vibration is observed as a broad peak around $3{,}400 \text{ cm}^{-1}$. A doublet peak at $2{,}905 \text{ cm}^{-1}$ explains the C–H symmetric and antisymmetric stretching of starch. A sharp peak at $1{,}650 \text{ cm}^{-1}$ is corresponding to the –OH bending vibration. A peak at $1{,}393 \text{ cm}^{-1}$ reveals the presence of C–H bending vibration. The C–O–C ether linkage of pyranose rings is observed at $1{,}025 \text{ cm}^{-1}$. The presence of ferrite nanoparticles can be confirmed by observing a peak at 587 cm^{-1} (Gang et al. 2010). Here, the peak corresponding to furosemide moieties is not observed due to the minimum quantity and the dominant FTIR peaks of starch. Figure 4b represents the FTIR spectrum of Fe_3O_4–furosemide–starch prepared under alkaline condition. Here also one can see the peaks corresponding to the –OH, C–H, –OH bending, C–O–C and M–O stretchings. The important peak noted here is the appearance of a new peak at $1{,}593 \text{ cm}^{-1}$ corresponding to the O^-Na^+ like ionic structure. It indicates that during the sodium hydroxide treatment all the –OH groups are converted into O^-Na^+ like structure. Further, the added sodium hydroxide stabilized the crystal structure of furosemide-functionalized ferrite as a nucleating agent. Figure 4c shows the FTIR spectrum of Fe_3O_4–furosemide–starch prepared under neutral pH. The present system also exhibits –OH, C–H, C–O–C and metal oxide stretching. The –OH bending vibration can be seen at $1{,}641 \text{ cm}^{-1}$. The C–H bending vibration is observed as a broad peak.

UV–visible spectroscopy

The UV–visible spectrum explains the possible electron transition in the chemical structure. Figure S1a is
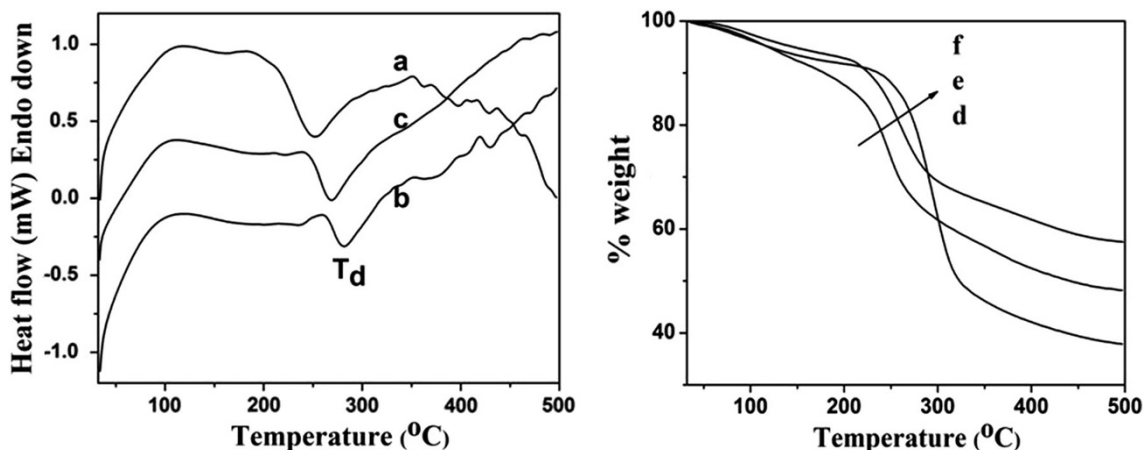
Fig. 5 DSC thermogram of ferrite–furosemide–starch synthesized under **a** acidic pH, **b** alkaline pH, **c** neutral pH and TGA of ferrite–furosemide–starch synthesized under **d** acidic pH, **e** alkaline pH, **f** neutral pH

responsible for the UV–visible spectrum of Fe_3O_4–furosemide–starch prepared under acidic pH. One broad hump at 277.8 nm is observed and corresponds to the $n \rightarrow \pi$ transition of the hydroxyl group. Fe_3O_4–furosemide–starch prepared under alkaline pH (Fig. S1b) exhibits two peaks. The first peak around 280 nm is corresponding to the $n \rightarrow \pi^*$ transition. The second small hump around 365 nm describes the presence of ferrite (Ahmad et al. 2009). The UV–visible spectrum of Fe_3O_4–furosemide–starch prepared under neutral pH (Fig.S1c). Peaks corresponding to Fig.S1a are also observed here. On thorough analysis, the UV–visible results indicated that Fe_3O_4 prepared under acidic pH simply degrade the ferrite structure. Hence, a peak corresponding to ferrite is absent in the spectrum.

DSC study

The DSC thermogram of Fe_3O_4–furosemide–starch prepared under three different pHs is shown in Fig. 5a–c. Starch treated under acidic pH exhibited the degradation temperature at 252 °C. Starch treated under alkaline pH shows the degradation temperature at 281.2 °C. The starch treated under neutral pH exhibited the same at 268.3 °C. On close comparison, starch treated at all pHs does not show the melting temperature. Above all, the starch treated under alkaline pH exhibited the highest degradation temperature due to the formation of ionic structure of starch; i.e., the formation of O^-Na^+ like ionic structure. Liu et al. (2009) studied the DSC of gelatinized starch. The T_g of starch was varied with the moisture content of the starch sample. In the present investigation, the T_g did not clearly appear due to the presence of chemical interaction between the starch and the hydrophilic furosemide-functionalized ferrite.

TGA profile

The thermal stability of starch treated at three different pHs in the presence of furosemide-functionalized ferrite is given in Fig. 5d–f. Figure 5d enumerates the TGA thermogram of starch treated under acidic pH. The thermogram exhibits a three-step degradation process. The first minor weight loss below 100 °C is associated with the removal of physisorbed water molecules. The second major weight loss up to 200 °C corresponds to the removal of chemisorbed water molecules. The third major weight loss around 270 °C is due to the breaking of intramolecular ether linkage, and the molecular weight of starch was suddenly decreased. After the degradation, it shows 38.5 % weight residue remains around 500 °C. Piyada et al. (2013) reported about the depolymerization of starch around 250–300 °C and led to the decrease in molecular weight of starch. Our results are merged with their reports. Figure 5e is corresponding to the degradation of starch treated in the presence of furosemide-functionalized ferrite under alkaline and neutral pHs, respectively. Here also one can observe a three-step degradation process with the percentage weight residue of 48.9 and 58.5 % around 500 °C, respectively (Fig. 5e, f). In overall comparison, the starch treated under acidic pH exhibited the lowest percentage weight residue, whereas the starch treated under neutral pH shows the highest percentage weight residue. Under acidic pH, the structure of ferrite was degraded and as a result exhibited the remaining lowest weight residue.

SEM history

The surface morphology of starch treated under acidic pH is shown in Fig. 6a. The morphology exhibited a broken stone-like surface due to the dispersion of nanoferrite. The diameter of the starch was determined as 9×10^{-6} m.
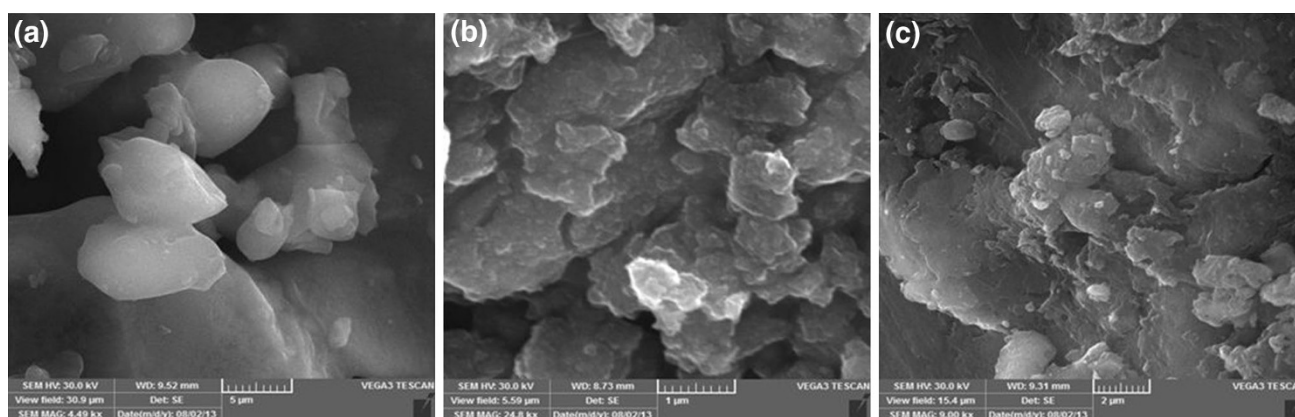
Fig. 6 SEM image of ferrite–furosemide–starch prepared under **a** acidic pH, **b** alkaline pH, **c** neutral pH
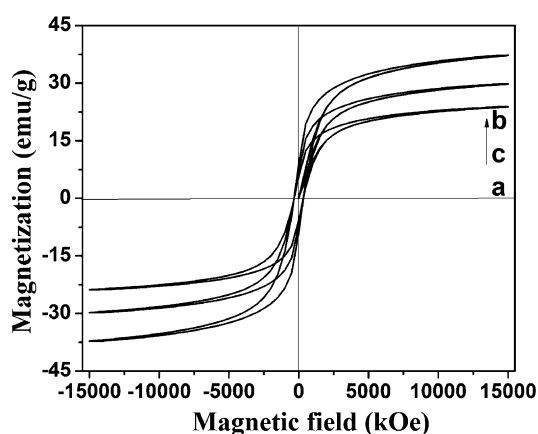

Fig. 7 VSM loops of ferrite–furosemide–starch prepared under **a** acidic pH, **b** alkaline pH, **c** neutral pH

Figure 6b defines the surface morphology of nanoferrite with broken stone-like morphology. The surface morphology of enzymatic hydrolyzed starch was found to be a broken stone-like surface morphology with microporous structure (Le Corre et al. 2012). Here, the size was determined as 1.5×10^{-6} m. This is due to the additional nucleation effect of NaOH. The surface morphology of starch treated under neutral medium in the presence of furosemide-functionalized ferrite is shown in Fig. 6c. Here also one can observe a broken stone-like morphology with the distribution of furosemide-functionalized ferrite. Under neutral medium, the size of ferrite was determined as 24×10^{-6} m. On comparison, the starch treated under NaOH medium exhibited the lowest size due to the nucleation and compact close-packing effects on starch induced by the added NaOH.

VSM study

The VSM value of starch/Fe$_3$O$_4$–furosemide system under different pH is given in Fig. 7. Figure 7a indicates the

VSM loop of starch/Fe$_3$O$_4$–furosemide system prepared under acidic condition, with the VSM value of 22.4 emu/g. Figure 7b, c represents the VSM loops of starch/Fe$_3$O$_4$–furosemide system prepared under alkaline and neutral pH with the magnetization values of 34.4 and 28.1 emu/g, respectively. Under alkaline pH, the ferrite gets nucleated and the size of ferrite gets reduced yielding a higher VSM value. In the case of acidic pH, the crystal structure of ferrite was degraded and yielded a low VSM value. On critical comparison with the pristine Ferrite, the nanocomposite system gave a lower value. This is due to the thin layer-like coating of starch on the surface of Ferrite (Vinod et al. 2008; Aouak et al. 2013). The sedimentation velocity of starch/Fe$_3$O$_4$–furosemide system under neutral pH exhibited the larger-size starch particles and settled down very fast with higher sedimentation velocity.

Sedimentation study

The sedimentation velocity of starch treated under three different pHs in the presence of furosemide-functionalized ferrite is described below. The sedimentation velocity of starch depends on the amount, charge, size and shape of the material. The furosemide-functionalized F$_3$O$_4$ concentration was varied between 0.5 and 1 % weight and indicated by a, b, c, d, and e, respectively. In the present investigation, the starch treated under neutral medium exhibited the highest sedimentation velocity of 12.415×10^{-6} m/s. This is due to the larger size of starch, and hence increases in gravitational force. Figure 8a indicates the effect of time on sedimentation height at five different concentrations. Figure 8b represents the plot of time against sedimentation height for the Fe$_3$O$_4$–furosemide–starch system treated under alkaline pH. The SEM analysis indicates that the size of starch was determined as 1.5×10^{-6} m, and hence the sedimentation velocity was found to be very low, i.e., 0.53×10^{-6} m/s. Figure 8c confirms the sedimentation
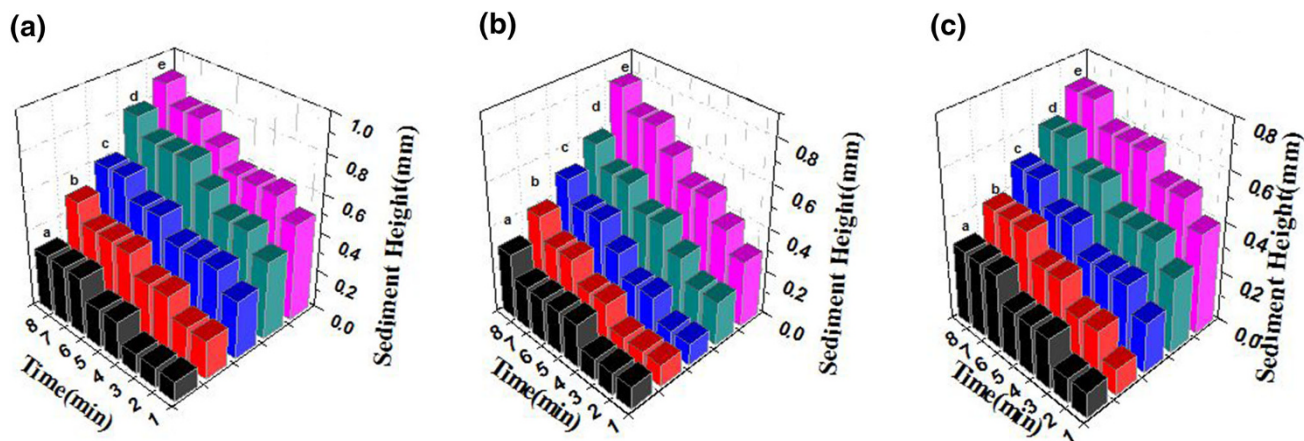
(a) **(b)** **(c)**

Fig. 8 Sedimentation height of ferrite–furosemide–starch system prepared under **a** acidic pH, **b** alkaline pH, **c** neutral pH at different concentrations

behavior of starch under neutral pH in the presence of furosemide-functionalized ferrite. Hence, the sedimentation velocity was calculated as 1.875×10^{-6} m/s. On comparison, it is found that the sedimentation velocity of starch depends on the size of the starch and pH of the medium. In the presence of the alkaline medium, the system exhibited the lowest sedimentation velocity. This is due to the absence of both inter- and intramolecular hydrogen bonding. Under alkaline pH, all the OH groups of starch were converted into O^-Na^+ like structures. But in the case of neutral pH, both inter- and intramolecular forces of attraction were not disturbed. Recently, Sajeev et al. (2002) studied the settling behavior of different starches under different experimental conditions. In the presence of surface-functionalized ferrite, the starch molecules settled very fast due to the combined effect of gravitational force, magnetic force and electrostatic interactions.

Conclusions

The niche points of the present investigation is summarized here as conclusion. The FTIR spectrum confirmed the surface-functionalized ferrite ($1,015$ cm^{-1}) by furosemide. The appearance of various crystal planes such as d_{311}, d_{400} and d_{533} in the XRD declared the formation of ferrite. After the surface functionalization of ferrite with furosemide, the VSM value was decreased to 42.7 emu/g. In the FTIR spectrum, a peak around 587 cm^{-1} confirmed the furosemide-functionalized ferrite nanoparticles in the starch/Fe$_3$O$_4$ nanocomposite system. The starch/Fe$_3$O$_4$ nanocomposite system under alkaline pH exhibited the highest thermal degradation temperature due to the formation of O^-Na^+ like ionic structure. Starch treated under neutral pH in the presence of furosemide-functionalized ferrite exhibited the highest

sedimentation velocity (12.415×10^{-6}m/s) due to the bigger size of the starch particles.

References

Ahmad S, Riaz U, Kashik A, Alam J (2009) Soft template synthesis of super paramagnetic ferrite nano particles a novel technique. J Inorg Organomet Polym 19:355–360

Aouak T, Deraz NM, Alarifi AS (2013) Synthesis, non-isothermal crystallization and magnetic properties of cobalt zinc ferrite/ poly(ethylene-co-vinylalcohol) nano composite. Bull Mater Sci 36:417–427

Bin WF, Jie C, Cong HK, Qin LS (2009) Preparation and electrochemical performance of spherical Fe$_3$O$_4$ as an anode material for Li-ion batteries. Sci China Ser E: Tech Sci 52:3219–3223

Chen BA, Zai YY, Wang XM, Cha NN (2008) Synergistic effect of the combination of nanoparticles Fe$_3$O$_4$ Au with daunomycin on K562/AO2 cells. Int J Nanomater 3(3):343–350

Closs CB, Petit BC, Roberts ID, Esher ID (1999) Phase separation and rheologies of aqueous starch/gallactomannan systems. Carbohydr Polym 39:67–77

Da G, Ferret F, Marechal PA, Thanch MC, Marouze ML, Dutour D (2010) Modeling small scale cassava starch extraction. Simulation of reduction of water consumption through a recycling process. Prog Biochem 45:1837–1842

Gang ZY, Yu SH, Dong PS, Qin HM (2010) Synthesis, characterization and preparation of ethylenediamine functionalized Fe$_3$O$_4$ magnetic polymers for the removal of Cr(iv) in wastewater. J Hazard Mater 182:295–302

He YP, Wang SQ, Li CR, Miao YM, Wu ZY, Zou BS (2005) Synthesis and characterization of functionalized silica coated

Fe$_3$O$_4$ superparamagnetic nanocrystals for biological applications. J Phys D: Appl Phys 38:1342–1350

Huang SH, Juang RS (2011) Biochemical and biomedical applications of multifunctionalized magnetite nanoparticles: a review. J Nanopart Res 13:4411–4430

Jiang L, Sun W, Kim J (2007) Preparation and characterization of Fe$_3$O$_4$ functionalized polystyrene magnetite nano composite. Mater Chem Phys 101:291–296

Kim MJ, Jang DH, Choa YH (2010) Preparation and characterization of carboxyl functionalisation of magnetic nanoparticles for oligo nucleotide immobilization. Phy Scr T139:1–4

Klokkenburg M, Hilhorst J, Erne BH (2007) Surface analysis of magnetite nanoparticles in cyclohexane solutions of oleic acid and oleylamine. Vib Spectrosc 43:243–248

Koussi GK, Wang P, Sreevatan S, Irudhayaraj J (2007) Aptamer mediated magnetite and gold coated magnetite nanoparticles as detection assay for prion protein assessment. Biotechnol Prog 23(1239):1244

Le Corre D, Vahanian E, Dufresne A, Bras J (2012) Enzymatic pretreatment for preparing starch nano crystals. Biomacromolecules 13:132–137

Li Z, Sun Q, Gao M (2005) Preparation of water soluble magnetic nanocrystals from hydrated ferrite salts in 2-pyrrolidine: meal leading to Fe$_3$O$_4$. Angew Chem 44:123–126

Liu P, Yu L, Liu H, Li L (2009) Glass transition temperature of starch studied a high speed DSC. Carbohydr Polym 77:250–253

Madariaga BC, Aquirre JA (2011) Combination treatment of corn starch waste water by sedimentation, microfiltration and reverse osmosis. Desalination 279:285–290

Mos SH, Shri S, Antwerp MV, Cao Z, Baker JR (2007) Dendrimer functionalized ironoxide nanoparticles for specific targeting and imaging of cancer cells. Adv Funct Mater 17:3043–3050

Piyada K, Waranyou S, Thawien W (2013) Mechanical, thermal and structural properties of rice starch reinforced with rice starch nano crystals. Int Food Res J 20:439–449

Prakash A, McCormick AV, Zachariah MR (2004) Aero-sol-gel synthesis of nanoporous iron oxide particles: a potential oxidizer for nano energetic materials. Chem Mater 16:1466–1471

Sajeev, Kaliappan R, NarayananVVS, Thangavel K (2002) Kinetics of gravity settling of cassava starch in aqueous suspension. Biosyst Eng 83(3):327–337

Sun J, Zhou S, Hou P, Yang Y, Li X, Li M (2007) Synthesis and characterization of bio-compatible Fe$_3$O$_4$ nanoparticle. J Biomed Mater Res A 80:333–341

Tian XZ, Wang JF, Qian SW, Wu WJ, Gang X (2010) Preparation and properties of F$_3$O$_4$ biomimetic micro-nano structure coatings. Adv Nat Sci 3(2):299–305

Vinod TP, Chang JH, Kim JW, Ree SW (2008) Self assembly and photopolymerization of diacetylene molecules on surface of magnetic nano particles. Bull Korean Chem Soc 29:799–804

Wei Y, Cheng S, Zheng Y (2008) Synthesis and floculating properties of cationic starch derivatives. Carbohydr Polym 74:673–679

Xiao ZP, Yang KM, Liang H, Lu J (2010) Synthesis of magnetic, reactive and thermo responsive F$_3$O$_4$ nanoparticle via surface initiated RAFT copolymerization of N-isopropyl-acrylamide and acrolein. J Polym Sci Part A: Polym Chem 48:542–550

Zhou Y, Wang S, Xie Y, Guang W, Dirz B, Yang Z, Jiang X (2008) 1, 3-dipolar cycloaddition as a general route for functionalization of F$_3$O$_4$ nanoparticle. Nanotechnology 19:1–5